Annales de Paléontologie 104 (2018) 217–229

Disponible en ligne sur
ScienceDirect
www.sciencedirect.com

Elsevier Masson France
EM|consulte
www.em-consulte.com

Original article

Rhinocerotidae (Mammalia, Perissodactyla) from the latest Oligocene Thézels locality, SW France, with a special emphasis on *Mesaceratherium gaimersheimense* Heissig, 1969

Rhinocerotidae (Mammalia, Perissodactyla) de l'Oligocène terminal de Thézels, Lot, avec un accent particulier sur Mesaceratherium gaimersheimense Heissig, 1969

Maxime Blanchon [a], Pierre-Olivier Antoine [b,*], Cécile Blondel [a], Louis de Bonis [a]

[a] *Laboratoire paléontologie évolution paléoécosystèmes paléoprimatologie, UMR 7262, Bât. B35 TSA 51106, 6, rue M.-Brunet, 86073 Poitiers cedex 9, France*
[b] *Institut des sciences de l'évolution, cc64, université de Montpellier CNRS, IRD, EPHE, place Eugène-Bataillon, 34095 Montpellier cedex 5, France*

ARTICLE INFO

Article history:
Received 28 February 2018
Accepted 25 May 2018
Available online 2 July 2018

Keywords:
Mesaceratherium gaimersheimense
Diaceratherium aff. *lemanense*
Oligocene-Miocene transition
Comparative anatomy
Biochronology

ABSTRACT

A taxonomic revision of the Rhinocerotidae from the latest Oligocene locality of Thézels in SW France is provided, based on comparative description of several hundreds of mandibular, dental, and postcranial specimens. In terms of abundance, the small-sized and slender-limbed rhinocerotine *Mesaceratherium gaimersheimense* Heissig, 1969 widely outnumbers the medium-sized and shorter-limbed teleoceratine *Diaceratherium* aff. *lemanense*. The material from Thézels in particular adds to the knowledge of *M. gaimersheimense* in providing for the first time valuable information on most elements of its appendicular skeleton, virtually unknown thus far. This work further confirms that *M. gaimersheimense* is restricted to the latest Oligocene interval, whereas *M. paulhiacense* (Richard, 1937) also first occurring in latest Oligocene deposits, survives during the earliest Miocene (Aquitanian standard age; Agenian European Land Mammal Age). The Agen area in SW France (type area of the Agenian ELMA) provides a well-documented sequence for latest Oligocene-earliest Miocene rhinocerotids of Western Europe with Thézels (MP30), Paulhiac (MN1), and Laugnac (MN2). *Mesaceratherium gaimersheimense* shows several postcranial differences with *M. paulhiacense* (shape of articular facets on central metapodials; slenderer astragalus but less slender metapodials) suggesting a still more cursorial locomotory mode for the latter species.

Mots clés :
Mesaceratherium gaimersheimense
Diaceratherium aff. *lemanense*
Transition Oligocène-Miocène
Anatomie comparée
Biochronologie

RÉSUMÉ

Une révision taxonomique des Rhinocerotidae de l'Oligocène terminal de Thézels (Bassin de la Garonne) est proposée, fondée sur la description comparative de plusieurs centaines de restes mandibulaires, dentaires et postcrâniens. En termes d'abondance, le petit rhinocérotiné *Mesaceratherium gaimersheimense* Heissig, 1969, aux membres très élancés, domine outrageusement l'autre forme reconnue, le téléocératiné *Diaceratherium* aff. *lemanense*, de taille moyenne et aux membres plus trapus. Le matériel de Thézels permet pour la première fois de décrire des éléments postcrâniens attribuables à *M. gaimersheimense*, dont les caractéristiques étaient jusqu'alors inconnues. Cette étude confirme par ailleurs que *Mesaceratherium gaimersheimense* disparaît du registre fossile à la limite Oligocène-Miocène, alors que *Mesaceratherium paulhiacense* (Richard, 1937), dont la plus ancienne mention remonte également à l'Oligocène terminal (MP30), remplace ce dernier au Miocène basal (Aquitanien/Agénien). La région d'Agen, dans le sud-ouest de la France (région type de l'étage mammalien Agénien), fournit une séquence très bien documentée pour les rhinocérotidés de l'intervalle Oligocène terminal – Miocène basal d'Europe occidentale, avec Thézels (MP30), Paulhiac (MN1), et Laugnac (MN2). *Mesaceratherium gaimersheimense*

* Corresponding author.
E-mail addresses: maxi_blan@hotmail.fr (M. Blanchon), pierre-olivier.antoine@umontpellier.fr (P.-O. Antoine), cecile.blondel@univ-poitiers.fr (C. Blondel), louisdebonis@univ-poitiers.fr (L. de Bonis).

https://doi.org/10.1016/j.annpal.2018.06.001
0753-3969/

présente quelques différences avec *M. paulhiacense* au niveau du postcrânien (astragale moins profond; disposition des facettes sur les métapodes centraux, eux-mêmes moins graciles) suggérant une meilleure adaptation à la course chez ce dernier.

1. Introduction

The Aquitaine Basin extends on about 40,000 square miles in southwestern France in a triangle limited by the Atlantic Ocean to the west, the Pyrenees to the South and the Massif Central to the Northeast. From Eocene times onward, fluvio-lacustrine deposits originating from the Massif Central and the Pyrenees accumulated and they preserved huge numbers of vertebrate remains (e.g., Richard, 1948). By the end of the Oligocene, sedimentation was mostly of detrital origin close to the Pyrenees and in the centre of the basin (molasses, marls, clays, sandstones) whereas lacustrine sedimentation deposited primarily in the northeastern edge of the basin (e.g., Cieurac limestone; Cavaillé, 1981). In the vicinity of the Thézels village, South of Cahors (Lot department, Fig. 1), the Cieurac limestone has yielded a lenticular body of marly deposits trapping a rich vertebrate fauna. A preliminary list of Thézels mammals was provided by Bonis and Guinot (1987), including rodents, a suoid (*Palaeochoerus* sp.), ruminants (*Dremotherium* cf. *Guthi* and *D.* cf. *quercyi*), rhinocerotids (*Diaceratherium* aff. *lemanense* and *Mesaceratherium* cf. *gaimersheimense*), a hyaenodontid (*Hyaenodon leptorhynchus*) and four species of amphicyonid (*Haplocyon* cf. *dombrowskii*, *Haplocyonopsis crassidens*, *Pseudocyonopsis landesquei*, and *Ysengrinia* sp.), hemicyonid (*Cephalogale* cf. *geoffroyi* and *Cephalogale* aff. *Bonali*), mustelid (*Plesictis genettoides* and *"Plesictis" milloquensis*), and ailurid carnivorans (*Amphictis* sp.), consistently pointing to a late Oligocene age for the locality (Arvernian European Land Mammal Age [ELMA]). The rodent assemblage includes *Eucricetodon thezelensis*, *Eucricetodon* sp.?, *Pseudocricetodon* sp., *Plesiosminthus admyarion*, *Plesiosminthus* sp.?, *Issiodoromys bransatensis*, *Adelomyarion vireti*, *Rhodanomys* aff. *transiens*, *Rhodanomys* sp.?, *Peridyromys murinus*, *Heteroxerus paulhiacensis*, and *Heteroxerus lavocati*, as revised by Comte (2000). These rodents have allowed for refining the age of Thézels, now unambiguously assigned to the MP30 reference level, late Arvenian ELMA, i.e., immediately prior to the Oligocene-Miocene transition (~23.03 Ma; Vandenberghe et al., 2012). We must note the lack of two genera normally present in MP 30, namely *Microbunodon* and *Archaeomys*. If not due either to paleoecological reasons or to a taphonomic bias, these absences could correspond to a level slightly younger than Coderet, the last reference level for the Oligocene epoch (MP 30).

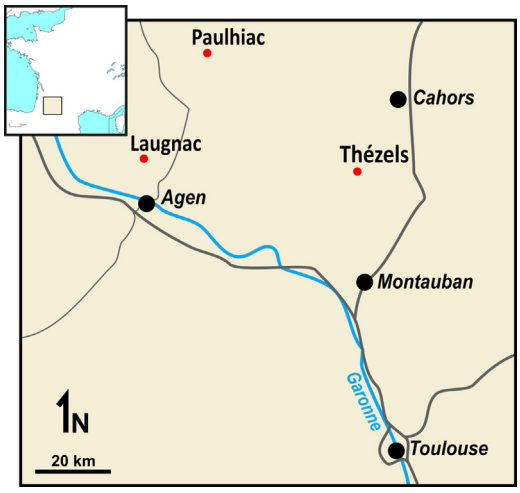

Fig. 1. Localization of Thézels (MP30) and Paulhiac (MN1), in the surrounding area of Cahors and Toulouse. Scale bar = 100 km.
Localisation de Thézels et Paulhiac, dans les environs de Cahors et Toulouse. Échelle = 100 km.

As suggested by Bonis and Guinot (1987), Thézels has yielded numerous cranio-mandibular, dental, and postcranial remains referable to two rhinocerotid species: the short-limbed teleoceratine *Diaceratherium* aff. *lemanense*, rare in the deposits (approximately 5%), and the long- and slender-limbed *Mesaceratherium* cf. *gaimersheimense* (95% in terms of specimen numbers). Remains assigned to *D.* aff. *lemanense* were thoroughly described by Michel (1983) and by Brunet et al. (1987). In this work, we will focus on specimens referable to the representative of *Mesaceratherium*, with a special emphasis on postcranial elements, which remained widely unknown so far.

2. Material and methods

2.1. Material

All Rhinocerotidae specimens from Thézels described here originate from two collections stored on CVCU (University of Poitiers, France). The so-called "old collection" (TheXXX; L. de Bonis' collection) corresponds to the remains collected during the excavations of the 1970s and 1980s with 446 cranio-mandibular, dental, and postcranial elements. The "new collection" (UP.TH.year.YYY) gathers remains collected by Master students (paleontology, University of Poitiers) in the last decade. This set includes around twenty cranial, dental and postcranial elements of Rhinocerotidae.

2.2. Comparison material

The rhinocerotid remains from Thézels were primarily compared to those assigned to Oligocene – earliest Miocene rhinocerotids from Europe, such as *Mesaceratherium* Heissig, 1969, *Diaceratherium* Dietrich, 1931, *Pleuroceros* Roger, 1898 and *Protaceratherium* Abel, 1910.

2.3. Methods

Capital letters are used for upper teeth (I, D, P, M), and lowercase letters for lower teeth (i, d, p, m). Dental terminology is that of Heissig (1972: pl. 13) and Antoine (2002) for rhinocerotids. The described anatomical features follow basically the same sequence as in Antoine (2002), and Antoine et al. (2010). Suprageneric systematics within Rhinocerotidae follows the arrangement proposed by Antoine et al. (2010) and Becker et al. (2013). Dimensions are given in mm.

2.4. Abbreviations

2.4.1. Anatomical abbreviations

Ant: anterior; APD: anteroposterior diameter; dist: distal; H: height; L: length; m.: musculus (muscle); max: maximum; Mc:

Metacarpal; min: minimum; Mt: metatarsal; post: posterior; TD: transversal diameter; W: width.

2.5. Localities

The, Thézels (MP30, Lot, France); Ph, Paulhiac (MN1, Lot-et-Garonne, France).

2.6. Institutions

CVCU Poitiers; Centre de Valorisation des Collections de l'Université de Poitiers.

3. Systematic palaeontology

Order Perissodactyla Owen, 1848.
Family Rhinocerotidae Gray, 1821.
Subfamily Rhinocerotinae Gray, 1821.
Tribe Rhinocerotini Gray, 1821.
Subtribe Teleoceratina Hay, 1902.
Genus ***Diceratherium*** Dietrich, 1931.
Type species: *Diceratherium tomerdingense* (Dietrich, 1931).
Referred species (our conception): *Diceratherium lemanense* (Pomel, 1853); *Diceratherium aurelianense* (Nouel, 1866); *Diceratherium asphaltense* (Depéret and Douxami, 1902); *Diceratherium aginense* (Répelin, 1917); *Diceratherium lamilloquense* Michel, 1983; *Diceratherium askazansorense* Kordikova, 2001. The generic assignment of the late early – early late Oligocene "Diceratherium massiliae Ménouret & Guérin, 2009" is here considered to be doubtful, notably as its hypodigm does not include any craniomandibular or dental elements.
Stratigraphic range: Late Oligocene – early Miocene (Late Arvernian – mid-Orleanian ELMA, MP29-MN4; Antoine and Becker, 2013; Scherler et al., 2013).

3.1. Diceratherium *aff.* lemanense

Most available elements have been already thoroughly described by Michel (1983) and Brunet et al. (1987). Only the specimens undescribed so far are studied here (mainly patellae).

3.1.1. Studied material

Right D4 fragment (The4045); distal right radius (The4336); patella fragment (The4244); patella fragment (The4245); right patella (The4246); patella fragment (The4247); patella fragment (The4248); right patella fragment (The4249); left patella fragment (The4411); distal left tibia (The4353).

3.1.2. Descriptions

Dental material

The fragmentary D4 (The4045) has small dimensions (Fig. 2A) (W = 32.6 mm; H = 18.7 mm). The distal side is broken with the distal border of the metaloph. The metaloph and the protoloph are linguo-distally oriented. A simple crista and a faint antecrochet are visible. A faint crochet is present on the apical part of the crown. The enamel is thin, especially on the lingual side of the ectoloph.

Postcranial material

The distal epiphysis of radius (The4336; Fig. 2B–C), shows three articular facets in distal view (Fig. 2B). The scaphoid-facet is deep and open anteriorly. The semilunate-facet and the pyramidal-facet are slightly concave sagittally and separate by a smooth ridge.

The patella (The4246) is thick, as high as wide and rhomboid (Fig. 2D). Muscular insertions are smooth, with the insertion of *m. fascia lata* visible on the anterior side. In proximal view, the insertion for the *m. vastus medialis* is marked.

Fig. 2. *Diceratherium* aff. *lemanense*, from the latest Oligocene of Thézels, France. Cranial, upper teeth and postcranial material. A. Fragment of right D4 (The4045) in occlusal view (Scale bar = 1 cm). B–C. Distal epiphysis of right radius (The4336) in distal (B) and anterior views (C) (Scale bar = 1 cm). D. Right patella (The4246), in anterior view (Scale bar = 1 cm). E. Distal end of left tibia (The4353) in posterior view. Scale bar = 2 cm
Diceratherium *aff.* lemanense *de l'Oligocène terminal de Thézels, France. Dents jugales supérieures et matériel postcrânien. A. Fragment de D4 droite (The4045) en vue occlusale (échelle = 1 cm). B–C. Épiphyse distale de radius droit (The4336) en vue distale (B) et antérieure (C). D. Patella droite (The4246), en vue antérieure (échelle = 1 cm). E. Extrémité distale de tibia gauche (The4353) en vue postérieure. Échelle = 2 cm.*

The distal end of the tibia (The4353) shows deep cochleae, especially for the lateral astragalus lip insertion (Fig. 2E). The posterior apophysis is high and rounded. The incomplete diaphysis is sagittally thick.

Discussion

Michel (1983) and Brunet et al. (1987) considered the Thézels diacerathere as documenting an early diverging morph of *D. lemanense*, being more "primitive" than the material from Gannat (type locality; MN1) and Paulhiac (MN1). Therefore, they assigned it to *D.* aff. *lemanense*. The postcranial material described here corroborates the picture of a massive and stocky rhinocerotid as evoked by Brunet et al. (1987) and Bonis and Guinot (1987). Nevertheless, limb bones are somewhat slenderer than the specimens from the type locality (Gannat; e.g., Boada-Saña et al., 2008; Becker et al., 2009). Therefore, pending a phylogenetically-constrained overview of diaceratheres, this material does not allow for precising further the taxonomic assignment of this teleoceratine and we prefer to leave it in open nomenclature.

3.2. Mesaceratherium gaimersheimense

Subfamily Rhinocerotinae, Gray, 1821.
Unnamed clade.
Genus ***Mesaceratherium*** Heissig, 1969.
Type species: *Mesaceratherium gaimersheimense* Heissig, 1969.
Included species: *Mesaceratherium paulhiacense* (Richard, 1937), *Mesaceratherium welcommi* Antoine and Downing, 2010.
Stratigraphical range: MP28-MN3 (Antoine et al., 2010; Antoine and Becker, 2013; Scherler et al., 2013).
Emended diagnosis

Medium-size hornless rhinocerotine, with a strong paracone fold on M1-M2, a posterior McIII-facet on McII, no posterior MtII-facet on MtIII, slender limbs, a transverse metaloph on P2, a lingual cingulum on lower premolars, and a curved magnum-facet on McII.

Mesaceratherium gaimersheimense, Heissig, 1969.

Emended diagnosis

Species with a protoloph occasionally interrupted on P2, protocone and hypocone separated on P2, no crochet on upper molars, a continuous metaloph on M1-M2 trigonid acute dihedron on lower cheek teeth and a superficial mediodistal gutter on tibia.

Differential diagnosis

Differs from *M. welcommi* by the absence of cement; a metacone without constriction on P3 and P4; no crochet on P3-P4; the connection entoconid-hypolophid on lower cheek teeth with lingual cingulum; closed diaphysis/olecranon angle; the calcaneus-facet 2 and calcaneus-facet 3 are independent on astragalus; and no fibula-facet on calcaneus. Differs from *M. paulhiacense* by its smaller size, a hypocone stronger than protocone on P2; upper molars with a marked labial cingulum; and the distal border on anterior face of the semilunate more rounded. Finally, differs from *M. welcommi* and *M. paulhiacense* by a hypocone-protocone separation on P2; and upper molars without crochet.

Referred material: see Supplementary Information for a complete list.

3.3. Descriptions

The studied sample is extremely consistent in terms of morphological features. Accordingly, characters found to be variable will be detailed in the descriptions.

3.3.1. Dental material

Twelve upper incisors are present in the remains (Table 1). The root of upper incisors is labially concave and shows a triangular cross-section, visible on the preserved right I1 (The4443; Fig. 3A–B). The elongated and flattened crown shows a slightly concave wear surface in the mesio-distal direction. No cingulum is visible on the upper incisors. The presence of I2 cannot be confirmed through the available material, but one specimen of I2 is present at Gaimersheim (Heissig, 1969).

The cheek teeth formula is 4P-3M, 4p-3m. The upper premolar series are long in comparison of molar series: $L_{P3-4}/L_{M1-3} \times 100 \approx 57$. Upper premolars are subquadrangular and show lingual and labial marked and continuous cingulum, visible on left maxilla (The4022; Fig. 3C–D) and right maxilla (The4023; Fig. 3E–F). The absence of crochet is notable. The postfossette is small but deep. Only one P1 (UP.TH.2016.005) was found at Thézels. This tooth is small (Table 1) with three roots and shows a protoloph, mesially inclined and separate from the ectoloph (Fig. 3G). The parastyle is mesially projected and lingually inclined. Labial and lingual cingula are continuous. Some P2 show a strong hypocone separate from the protocone, but no antecrochet. The metaloph is subtransverse and the protoloph is directed distally. The ectoloph and the protoloph are connected.

The protocone on P3 has no constriction but a connection with the hypocone forming a thin lingual bridge. The metaloph is disto-lingually inclined. The central valley is simple, without crista, pseudo-metaloph, or antecrochet. The P4, larger than other premolars (Table 1), is like P3 in having an unconstricted protocone connected to the hypocone, the metaloph disto-lingually inclined and a simple central valley. Upper molars, likewise with a subquadrangular occlusal surface, show a thin labial cingulum. The distal cingulum is also marked over the entire width, except for M3. The central valley structure is simple, with only an antecrochet and a crochet (only in upper part of the crown on the M3). Both the medifossette and the crista are missing on upper molars.

All M1s show a paracone with a strong fold and a markedly constricted protocone. The metaloph is continuous and does not show a fold. M1s also show a lingual groove of the protocone, absent on M2. M2 shows a similar morphology, although slightly larger (Table 1). The metastyle is elongate and the posterior profile of the ectoloph is concave. The distal cingulum is present and continuous. No junction between antecrochet and crochet is present on M1 and M2 (Fig. 3D and F). The cristella and the mesostyle are absent on these teeth. Finally, M1 and M2 show a deep reduced post-fossette. M3 have a quadrangular outline in occlusal view, yet with a metaloph and an ectoloph fused into an ectometaloph. The protoloph is transverse and the protocone is not constricted. There is no posterior groove on ectometaloph.

Table 1
Mesaceratherium gaimersheimense Heissig, 1969 and *Diaceratherium* aff. *lemanense* from Thézels, latest Oligocene, SW France.
Mesaceratherium gaimersheimense *Heissig, 1969 et* Diaceratherium *aff.* lemanense *de Thézels, Oligocène terminal, Sud-Ouest de la France.*

Tooth	L		Wmax		H
	M. g.	*D.* aff. *l.*	*M. g.*	*D.* aff. *l.*	*M. g.*
I1	30.8–42.6; 35.5 [6]	–	10.9–14.6; 13.1 [6]	–	48–57.6; 54.8 [5]
P1	20 [1]	–	18.5 [1]	–	12.9 [1]
P2	20–25.6; 23.2 [7]	–	28–32; 29.5 [7]	–	15–20.8; 18.5 [5]
P3	26–27.7; 26.6 [6]	–	33.6–36.7; 35.1 [6]	–	20–26; 23.1 [6]
P4	27–3; 30.1 [6]	–	38.6–46; 40.8 [6]	–	21.9–29.7; 25 [5]
M1	31–34.6[b]; 32.0 [4]	–	38.7–43.4; 41.5 [5]	–	19.7–26.3; 25.3 [4]
M2	32–36.3; 33.8 [5]	–	43.4–46; 44.7 [5]	–	26–30; 28.4 [5]
M3	32.3–36; 33.3 [4]	–	40–45; 42.4 [4]	–	23.5–30; 27.1 [4]
d1	–	–	–	–	–
d2	21–23.7; 22.35 [2]	–	11.4–13; 12.2 [2]	–	–
d3	32–33; 32.4 [3]	–	15–18; 16.1 [3]	–	–
d4	29.6–31.6; 30.6 [3]	–	17.4–19.7; 18.3 [3]	–	–
p1	15.3–17; 16.2 [5]	–	8–9.6; 9 [5]	–	11–13.4; 11.9 [5]
p2	20.6–23.6; 22.1 [4]	25[a] [1]	11.8–15.5; 13.8 [4]	17[a] [1]	11.6–21; 16.3 [2]
p3	27–30.3; 28.2 [4]	31[a] [1]	19.4–22; 20.6 [6]	23[a] [1]	18–25; 22.5 [4]
p4	27.6–33; 30.6 [7]	35[a] [1]	21–23.9; 22.7 [7]	25.5[a] [1]	18.7–28; 23.8 [7]
m1	30–33.7; 31.6 [8]	40.5[a] [1]	20.5–24; 22.8 [8]	26[a] [1]	20.2–24.6; 22.1 [7]
m2	31.5–38; 34.7 [10]	46–48; 47 [2]	23–26; 24.5 [10]	29; 29 [2]	17–25.7; 22.7 [8]
m3	33–39; 36.2 [5]	45.5–46; 45.75 [5]	21.3–22.7; 22.3 [6]	28; 28 [2]	15–27; 21 [4]

Dental dimensions, in mm: range; mean [number of specimens]; H: crown height; L: Length; max: maximal; W: Width; *M. g.*: *Mesaceratherium gaimersheimense*; *D.* aff. *l.*: *Diaceratherium* aff. *lemanense*.

[a] Measurements taken from Michel (1983).

[b] Estimated value.

Fig. 3. *Mesaceratherium gaimersheimense* Heissig, 1969, from the latest Oligocene of Thézels, France. Cranial material and upper teeth. A–B. Left I1 (The4443) in lingual (A) and occlusal views (B). C–D. Fragment of a left maxilla with P2-M3 (The4022) in labial (C) and occlusal views (D). E–F: Fragment of a right maxilla with P2-M2 and damaged M3 (The4023) in labial (E) and occlusal views (F). Scale bar = 2 cm. G. Right P1 (UP.TH.2016.005) in occlusal view (scale bar = 1 cm).
Mesaceratherium gaimersheimense Heissig, 1969, de l'Oligocène supérieur de Thézels, France. Matériel crânien et dents jugales supérieures. A–B. I1 gauche (The4443) en vue linguale (A) et occlusale (B). C–D. Fragment de maxillaire gauche avec P2-M3 (The4022) en vue labiale (C) et occlusale (D). E–F. Fragment de maxillaire droit avec P2-M2 et M3 endommagée (The4023) en vue labiale et occlusale (F). Échelle = 2 cm. G. P1 droite (UP.TH.2016.005) en vue occlusale (échelle = 1 cm).

Fig. 4. *Mesaceratherium gaimersheimense* Heissig, 1969, from the latest Oligocene of Thézels, France. Cranial material and lower teeth. A–B. Left mandible from a juvenile with d2-d4 and preserved ramus (The4004) in lingual (A) and occlusal views (B). C. Right i1 (The4076) in lateral view (scale bar = 1 cm). D. Right i2 (The4088) in labial view. E-F. Right p1 (The4307) in labial (E) and occlusal (F) views (scale bar = 1 cm). G–H. Fragment of a right mandible with p3-m3 (The4021) in lingual (G) and occlusal views (H); I, subcomplete mandible with left p2-p4/m2-m3 and right p3-p4 and m3 (UP.TH.2016.011) in occlusal view. J. Fragment of a left mandible with p4-m3 (The4009) in labial view. Scale bar = 2 cm.
Mesaceratherium gaimersheimense *Heissig, 1969, de l'Oligocène terminal de Thézels, France. Matériel crânien et dents jugales inférieures. A–B. Mandibule droite avec d2-d4 et ramus préservé (The4004) en vue linguale (A) et occlusale (B). C. I1 droite (The4076) en vue latérale (échelle = 1 cm). D. 12 droite (The4088) en vue labiale. E-F. P1 droite (The4307) en vue labiale et occlusale (F) (échelle = 1 cm). G–H. Fragment de mandibule droite avec p3-m3 (The4021) en vue linguale (G) et occlusale (H). I. Mandibule subcomplète avec p2-p4/m2-m3 gauche et p3-p4 and m3 droite (UP.TH.2016.011) en vue occlusale. J. Fragment de mandibule gauche avec p4-m3 (The4009) en vue labiale. Échelle = 2 cm.*

The slender mandible (The4004) shows d2-d4 with small dimensions (Fig. 4A–B, Table 1). This d2 has a spur-like paralophid, expanded on the mesial side. The anterior groove on the entoconid is present, and the posterior valley is closed. On d3 (Fig. 4B), the paralophid is split and the metaconid shows a low constriction. Finally, d4 is molar-like (Fig. 4B).

The right i1 (The4076; Fig. 4C) shows a single root and a globular crown, without cingulum.

All i2s are erected in tusk. On i2 The4088, the crown section is triangular (Fig. 4D), sharpened on mesial side and the lingual side is slightly concave (Table 1). No cingulum is visible on specimens. The p1 (The4307; Fig. 4E–F) has only one root and shows labial and lingual continuous cingulum. Protoconid and paraconid are marked with no bifurcation. The posterior valley is closed, except on The4075. All p2s show a paralophid, projected like a spur and isolated by two grooves. The posterior valley is lingually open (Fig. 4G–H). The lingual cingulum is reduced and the labial cingulum is continuous, marked in thin strip. On molariform p3 and p4 (Fig. 4G–I), cingula are like on p2, i.e., reduced on the lingual side and continuous on the labial side. The ectolophid groove is angular and vanishing before the neck. The trigonid is angular and it forms a right dihedron. The metaconid is connected to the metalophid, and the entoconid is connected to the hypolophid. The opening of posterior valley is V-shaped. Molars are simple and like premolars (Table 1), with cingula reduced on lingual side and continuous on labial side. However, on m3, there is no visible cingulum, except on the mandible (The4009; Fig. 4J). The ectolophid groove is angular and vanishing before the neck. The trigonid is angular in right dihedron. The metaconid is connected to the metalophid and entoconid is connected to the oblique hypolophid. There is no lingual entoconid groove.

3.3.2. Mandibular material

On the complete mandible (UP.TH.2016.011, Fig. 4I), the symphysis is massive, like a platform along the corpus mandibulae. Its posterior side reaches p3. No foramen mentale is preserved. The base of the corpus mandibulae on (The4021) and (UP.TH.2016.011) is straight.

Table 2
Mesaceratherium gaimersheimense Heissig, 1969 and *Diaceratherium* aff. *lemanense* from Thézels, latest Oligocene, SW France.
Mesaceratherium gaimersheimense *Heissig, 1969 et* Diaceratherium aff. lemanense *de Thézels, Oligocène terminal, Sud-Ouest de la France.*

		Prox. epiphysis		diaphysis		Dist. epiphysis				
	L	TD	APD	TD mini	APD	TD	APD	Humerus: TD deltoid tuberosity	McII: TD prox art.	McII and McIII: TD dist. Art.
Humerus										
M. g.	298.1	109.8	–	39.2–49.9; 42.7 [4]	44.7–49.4; 45.5 [3]	82.2–99.1; 89.4 [5]	68–73.2; 70.6 [2]	77.6–83.2; 80.4 [2]	–	–
D. aff. *l.*	415–432[a]; 423.5 [2]	182.7–184.2; 183.5 [2]	–	53.6–63.1; 58.4 [2]	–	125.7–131.8; 128.8 [2]	80.9	119.1–135; 127.1 [2]	–	–
Radius										
M. g.	–	60.9–70; 65.4 [5]	34.7–38.2; 36.5 [2]	–	–	70.8	–	–	–	–
D. aff. *l.*	–	–	–	–	–	–	–	–	–	–
McII										
M. g.	140.3	28–29.2; 28.5 [3]	19–22.3; 20.7 [3]	23–25; 24.3 [3]	10.2–12.6; 11.5 [3]	28.5	24.7	-	23.8–25.8; 25 [3]	25.2
D. aff. *l.*	–	–	–	–	–	–	–	–	–	–
McIII	153–172.9; 165.2 [7]	32.1–40.5; 38.6 [9]	22.3–32; 28.1 [9]	30.2–37.8; 32.9 [8]	11.8–15; 13.6 [8]	40.3–50.7; 42.9 [7]	25–29.5; 26.5 [7]	–	–	31.1–45; 36.7 [7]
M. g.										
D. aff. *l.*	171[a]	54–57.3; 55.7 [2]	31.4–36.3; 33.9 [2]	48[a]	19	57.5	42.3	–	–	46

Compared dimensions of anteriors stylopods, zeugopods and metapods, in mm: range; mean [number of specimens]; L: Length; TD: Transversal Diameter; APD: Anteroposterior Diameter; prox: proximal; dist: distal; mini, minimum; art: articulation; *M. g.*: *Mesaceratherium gaimersheimense*; *D.* aff. *l.*: *Diaceratherium* aff. *lemanense*.

[a] Measurements taken from Michel (1983).

Fig. 5. *Mesaceratherium gaimersheimense* Heissig, 1969, from the latest Oligocene of Thézels, France. Postcranial material. A. Right humerus (The4322) in posterior view. B. Proximal epiphysis of right radius (The4329) in anterior view. C. Distal epiphysis of left radius (The4335) in distal view. D. Left ulna (The4338) in lateral view. E. Right scaphoid (The4208) in postero-lateral view. F–G. Left semilunate (The4191) in anterior (F) and lateral views (G). H. Left pyramidal (The4169) in medial view. I. Right pisiform (The4462) in lateral view. J. Right trapezoid (The4235) in medial view. K. Right magnum (The4172) in lateral view. L. Right unciform (The4219) in medial view. M. Right McII (The4124) in lateral view. N–O. Left McIII (The4133) in anterior (N) and proximal views (O). P–Q. Proximal half of right McIV (The4117) in lateral (P) and proximal views (Q). Scale bar = 1 cm.
Mesaceratherium gaimersheimense *Heissig, 1969, de l'Oligocène terminal de Thézels, France. Matériel postcrânien. A. Humérus droit (The4322) en vue postérieure. B. Épiphyse proximale de radius droit (The4329) en vue antérieure. C. Épiphyse distale de radius gauche (The4335) en vue distale. D. Ulna gauche (The4338) en vue latérale. E. Scaphoïde droit (The4208) en vue postérieure. F–G. Semi-lunaire gauche (The4191) en vue antérieure (F) et latérale (G). H. Pyramidal gauche (The4169) en vue médiale. I. Pisiforme droit (The4462) en vue latérale. J. Trapézoïde droit (The4235) en vue médiale. K. Magnum droit (The4172) en vue latérale. L. Unciforme droit (The4219) en vue médiale. M. McII droit (The4124) en vue latérale. N–O. McIII gauche (The4133) en vue antérieure (N) et proximale (O). P–Q. Moitié proximale de McIV droit (The4117) en vue latérale (P) et proximale (Q). Échelle = 1 cm*

3.3.3. *Postcranial skeleton*

The material is composed of 270 specimens, essentially limb bones.

Regarding the humerus, most elements are proximal and distal fragments, but two complete humeri are available (The4322 and The4436). The humerus (The4322) is slender (Fig. 5A; Table 2). The proximal epiphysis shows an oval humeral head, but the lateral side is missing (encompassing great tuberosity and secondary tubers). On the distal epiphysis, the lateral epicondyle is narrow. The trochlea is egg cup-shaped. No trochlear scar is present. The fossa olecrani is high and the coronoid fossa is oval and deep.

Only proximal and distal fragments of radius are available but the preserved parts point to a long and slender bone (Table 2). The right proximal epiphysis (The4329) has a wide glenoid cavity, oblique medio-distally in anterior view and slightly concave sagittally (Fig. 5B). The anterior border (like the medial border of the shaft) is straight. The insertion for the m. biceps brachii is superficial. The distal epiphysis (The4335, Fig. 5C) has a scaphoid-facet sigmoid in cross section (convex anteriorly and concave posteriorly). The large semilunate-facet is concave transversely and the pyramidal-facet forms a thin narrow oblique strip.

One complete ulna is preserved (The4338). It is long and slender (Fig. 5D). The proximal epiphysis (APD = 112.6 mm) has a long olecranon process. The synovial notch is marked, split into V-shaped facets for the humerus. The coronoid process and the facets for the radius are damaged. The diaphysis is eroded (TD = 25.2 mm; APD = 46.5 mm). The angle between the diaphysis and the olecranon is around 135°. There is only one crescent-like distal facet for the radius. The pyramidal-facet is concave in frontal view.

The scaphoid is elevated but thick transversely (The4208; Table 3; Fig. 5E). Its posterior height slightly exceeds the anterior height. The proximal view shows a triangular facet for the radius, latero-medially concave with a posterior tip. The lateral side shows two slightly erased facets for the semilunate. The medial side has salient tuberosity in its posterior part. In distal view, the magnum facet is sagittally concave and transversally flat. However, the trapezoid-facet is sagittally concave and transversally convex, extending on medial side. The trapezium-facet is wide and rhomboid.

In proximal view, the semilunate (The4191) has a sagittally convex facet for the radius, with a large and shallow gutter juxtaposed on its distal side (Fig. 5F–G). The anterior side also has a keeled median tuberosity and a sharp tip. The medial side shows two scaphoid-facets, elongated sagittally. The distal facet for the scaphoid is crescent shaped. The magnum-facet is flat or slightly concave and elongated proximo-distally. The lateral side shows a concave unciform-facet and two small pyramidal-facets.

The pyramidal (The4169, Fig. 5H) is elevated and narrow. The ulna-facet is laterally inclined and rhomboid in proximal view, with a curved tip posteriorly directed in lateral view (Table 3). The lateral side shows a pisiform-facet contiguous to the ulna-facet. The medial side bears two semilunate-facets. The proximal one is half-moon shaped. The distal facet is asymmetric and comma-like. In distal view, the unciform-facet is triangular and concave anteroposteriorly.

The pisiform is elongated anteroposteriorly (The4462; L = 49.4 mm; W = 35.5 mm) and spatulate posteriorly (H = 21.6 mm). The pyramidal-facet is curved. The ulna facet is subrectangular and slightly concave latero-medially. The lateral side is rough and convex. The medial side is smooth and concave (Fig. 5I).

The trapezoid is elevated (Table 3). On The4235, the scaphoid-facet has asymmetric borders (Fig. 5J). This facet and the McII-facet are strongly concave in lateral view. The magnum-facet on the lateral side is flat and reduced. The trapezium-facet is flat, filling the entire medial side.

The magnum is high and developed sagittally (The4172; Table 3), with an anterior pad oriented proximally. The proximal border of the anterior side is straight or nearly straight in anterior view. In proximal view, the scaphoid-facet is concave and connecting the slightly concave unciform-facet, forming a dihedral edge. This unciform-facet extends on the lateral side. The articular process for the semilunate is semicircular in lateral view (Fig. 5K). A strongly concave McIII-facet is visible in distal view. The indentation between the medial facets is shallow. The posterior tuberosity is long and straight, transversely compressed.

The unciform is high and wide (The4219; Table 3; Fig. 5L). Proximally, the semilunate- and the pyramidal-facets are strongly convex sagittally. In anterior view, they connect at a right angle. The pyramidal- and McV-facet are remote. The latter is oblique (∼50° with the horizontal line), thus pointing to a possible tetradactyl

Table 3
Mesaceratherium gaimersheimense Heissig, 1969 from Thézels, latest Oligocene, SW France.
Mesaceratherium gaimersheimense, *1969 de Thézels, Oligocène terminal, Sud-Ouest de la France.*

				Scaphoid: Prox articulation		Scaphoid: Dist articulation			
	L	W	H	L	W	L	W	Scaphoid: palmar H	Semilunate: TD Unciform articulation
Scaphoid	55.5–62.1; 59.1 [3]	30.8–35.3; 32.2 [5]	48.6–54.7; 51.3 [6]	19.7–25.5; 22.2 [6]	28.9–34; 31.1 [4]	31.3–34.6; 33.0 [2]	18.1–23.4; 20.4 [3]	38–39.9; 38.8 [4]	–
Semilunate	57.9–67.9; 60.7 [6]	32.6–40.6; 34.4 [7]	40.8–44.7; 42.0 [8]	–	–	–	–	–	23–31.8; 27.0 [8]
Pyramidal	23–29; 27.2 [5]	37.1–42; 39.9 [4]	41.3–51.2; 43.9 [5]	–	–	–	–	–	
Trapezoid	22.8–29.8; 26.2 [4]	13.9–20.5; 18.0 [4]	22–26.4; 24.9 [4]	–	–	–	–	–	
Magnum	62.2–71.2; 67.0 [5]	25.4–35.8; 28.7 [5]	45.1–52.1; 48.9 [7]	–	–	–	–	–	
Unciform	60.4–65.4; 63.2 [6]	42.6–50.9; 47.2 [11]	34.8–42.8; 38.4 [10]	–	–	–	–	–	

Dimensions of carpal bones, in mm: range; mean [number of specimens]; L: Length; W: Width; H: Height; TD: Transversal Diameter; prox: proximal; dist: distal.

Table 4
*Mesaceratherium gaimersheimens*e Heissig, 1969 and *Diaceratherium* aff. *lemanense* from Thézels, Late Oligocene, SW France.
Mesaceratherium gaimersheimense *Heissig, 1969 et* Diaceratherium *aff.* lemanense *de Thézels, Oligocène terminal, Sud-Ouest de la France.*

		Prox. epiphysis		diaphysis		Dist. epiphysis			Femoral head		Third trochanter	
	L	TD	APD	TD mini	APD	TD	APD	TD dist. Art.	TD	APD	H	TD
Femur												
M. g.	381.8–390; 385.9 [2]	126.7–147; 135.5 [3]	–	50–57.8; 54.2 [4]	30.6–33.2; 31.8 [4]	85.5–94.8; 90.3 [4]	77–115.3; 99.2 [4]	–	56.4–57.4; 56.7 [4]	42.2–54; 50 [3]	31.4–41; 36.2 [2]	73.5–86.3; 78 [4]
D. aff. *l.*	490[a]	–	–	–	–	–	–	–	–	–	–	–
Tibia												
M. g.	290.2	76.1–100.7; 86.2 [4]	83	40.5–46.3; 42.7 [3]	31.3–31.6; 31.5 [2]	63.6–74; 64.1 [3]	42–45.5; 44.2 [3]	–	–	–	–	–
D. aff. *l.*	–	–	–	–	–	85.7	65.8	–	–	–	–	–
Patella												
M. g.	63.1–68.3; 65.2 [2]	60.9	28.6–29.4; 29 [2]					–	–	–	–	–
D. aff. *l.*	60.2–70.4; 65 [4]	60.4	38.8					–	–	–	–	–
MtIV												
M. g.	134	25.2–28.5; 27.4 [4]	24–33.3; 28.4 [4]	16	25.4	41	25.6	–	–	–	–	–
D. aff. *l.*	124–125[a]; 124.5 [2]	42[a]	37[a]	21.6	25.7	–	33–37.5[a]; 35.3 [2]	32–34[a]; 33 [2]	–	–	–	–

Compared dimensions of posteriors stylopod, zeugopod and metapods, in mm: range; mean [number of specimens]; L: length; TD: transversal diameter; APD: anteroposterior diameter; prox: proximal; dist: distal; mini: minimum; *M. g.*: *Mesaceratherium gaimersheimense*; *D.* aff. *l.*: *Diaceratherium* aff. *lemanense*.

[a] Measurements taken from Michel (1983).

Table 5
Mesaceratherium gaimersheimense Heissig, 1969 and *Diaceratherium* aff. *lemanense* from Thézels, latest Oligocene, SW France.
Mesaceratherium gaimersheimense *Heissig, 1969 et* Diaceratherium *aff.* lemanense *de Thézels, Oligocène supérieur, SW France.*

				dist. art.						
	H	TD	APD int	TD	APD	DL	TD max dist.	APD	TD/H	APD/H
M. g.	54.8–63; 59.3 [13]	53.8–66.8; 60.9 [12]	29–43.5; 36.8 [14]	45.4–53.9; 51.4 [9]	25.2–32.9; 29.1 [9]	39.1–42.6; 40.9 [13]	52.1–61.5; 53.7 [8]	35–42.4; 38.3 [7]	0.94–1.13; 1.03 [12]	0.59–0.71; 0.64 [7]
D. aff. *l.*	75.5[a]	83[a]	51	73[a]	44.8	60[a]	52.7	54.8	1.09	0.726

Compared dimensions of astragali, in mm: range; mean [number of specimens]; H: Height; dist.: distal; art.: articulation; TD: Transversal Diameter; APD: Anteroposterior Diameter; max: maximum; APD int: APD of medial lip of the trochlea; DL: distance between lips; *M. g.*: *Mesaceratherium gaimersheimense*; *D.* aff. *l.*: *Diaceratherium* aff. *lemanense*.

[a] Measurements taken from Michel (1983).

Fig. 6. *Mesaceratherium gaimersheimense* Heissig, 1969, from the latest Oligocene of Thézels, France. Postcranial material. A. Right femur (The4437) in postero-lateral view. B–C. Proximal epiphysis of right tibia (The4463) in lateral (B) and proximal views (C). D. Distal half of left tibia (The4351) in anterior view. Scale bar = 4 cm. E. Left patella (The4441) in anterior view. F–G. Left astragalus (The4151) in anterior (F) and posterior views (G). H. Right calcaneus (The4162) in lateral view. I. Right navicular (UP.TH.2016.006) in distal view. J–K. Right ectocuneiform (The4232) in proximal (J) and distal views (K). L. Left cuboid (The4182) in medial view. M–N. Proximal epiphysis of right MtIII (The4304) in anterior (M) and proximal views (N). O–P. Fragment of proximal epiphysis of right MtIV (The4135) in medial (O) and proximal views (P). Scale bar = 1 cm.
Mesaceratherium gaimersheimense *Heissig, 1969, de l'Oligocène terminal de Thézels, France. Matériel postcrânien. A. Fémur droit (The4437) en vue postérieure. B-C. Épiphyse proximale de tibia droit (The4463) en vue latérale (B) et proximale (C). D. Moitié distale de tibia gauche (The4351) en vue antérieure. Échelle = 4 cm. E. Patella gauche (The4441) en vue antérieure. F-G. Astragale gauche (The4151) en vue antérieure (F) et postérieure (G). H. Calcanéum droit (The4162) en vue antérieure. I. Naviculaire droit (UP.TH.2016.006) en vue distale. J-K. Ectocunéiforme droit (The4232) en vue proximale (J) et distale (K). L. cuboïde droit (The4182) en vue médiale. M-N. Épiphyse proximale de MtIII droit (The4304) en vue antérieure (M) et proximale (N). O-P. Fragment d'épiphyse proximale de MtIV droit (The4135) en vue médiale (O) et proximale (P). Échelle = 1 cm.*

manus following Antoine and Welcomme (2000) and Antoine (2002). The posterior tuberosity is slightly longer than the articular part. The distal facet presents a set of concave articular facets, corresponding to the McIII, McIV, and McV.

All available metacarpals are slender (Table 3). They are narrow, elongated dorsoventrally, and sagittally flattened. The McII has a proximal epiphysis with a trapezoid-facet convex sagittally and slightly concave transversely. The magnum-facet is curved in lateral view, forming a thin strip (Fig. 5M). This facet is connected to the trapezoid-facet. The trapezium- and McIII-facets are damaged on all available specimens. Distally, the intermediate relief is low and smooth.

Seven complete McIIIs are preserved (The4096, The4097, The4098, The4106, The4121, The4122, and The4133) and two proximal fragments (The4109 and The4130). The proximal epiphysis is hardly wider than the diaphysis. The magnum-facet is sagittally concave, convex transversely, and elongated anteriorly (Table 3). In proximal view, the unciform-facet is triangular, flat and inclined laterally. In lateral view, two flat McIV-facets are separate by a gutter. On the anterior side, the insertion of the m. extensor carpalis is flat (Fig. 5N–O). The diaphysis is widened distally. Mean Gracility Index equals 20.1. Intermediate relieves are eroded on all available specimens.

Only one proximal epiphysis of McIV is available (The4117; TD = 23 mm; APD = 31.7 mm). The unciform-facet is triangular and elongated sagittally (Fig. 5P–Q). Other features are not observable, due to erosion.

No McV is preserved.

Two complete femora (The4437 and The4438) and several epiphyses have been collected. The femur is slender with a thin diaphysis (Fig. 6A). The head is hemispheric (without medial stiff). The fovea capitis is damaged. The trochanter major is not preserved, but the third trochanter is developed (Table 4). Furthermore, the lesser trochanter is present and elongated as a thin lamina reaching the femoral head. The distal part shows a deep intercondylar fossa (visible on The4347), delimited by two marked condyles. The trochlea forms a 135° angle with the diaphysis and the medial lip of the proximal trochlea is elongated proximally. The lateral lip shows a light elongated mark on the inner side, visible on (The4438).

One complete tibia (with the proximal half in bad condition), two proximal epiphyses, and three distal ends of tibia are available. They are long and slender (Table 4). The proximal femur-facets are damaged and the intercondylar eminence is eroded. Two ligament notches are visible from either sides of the tibial tuberosity in proximal view (Fig. 6B–C). The lateral ligament notch corresponds to the anterodistal groove, as indicated by Antoine (2002). The distal end (The4351; Fig. 6D) shows a deep mediodistal gutter. The posterior apophysis is high and sharp.

The patella is lozengic in anterior view (Fig. 6E) and as high as wide (Table 4). Muscular insertions are smooth on the anterior side, except for (The4441), probably belonging to an aged individual. The most prominent insertion is for the *M. gluteo-biceps*.

Twenty-seven astragali are preserved (Fig. 6F–G). Their dimensions are similar (Table 5), being high and slender (TD/H = 1.03; APD/H = 0.64). The fibula-facet is subvertical and flat. The collum tali is high. The postero-proximal border of the trochlea is nearly straight and the trochlea is oblique with respect to the distal articulation. The lateral lip is more prominent than the medial lip. Three calcaneus-facets are visible on the posterior side. The calcaneus-facet 1 is deeply concave in the sagittal plane. It has a high and

Table 6
Mesaceratherium gaimersheimense Heissig, 1969 and *Diaceratherium* aff. *lemanense* from Thézels, latest Oligocene, SW France.
Mesaceratherium gaimersheimense *Heissig, 1969 et* Diaceratherium *aff.* lemanense *de Thézels, Oligocène terminal, Sud-Ouest France.*

	H	APD top	APD beak	TD sust.	TD top	TD mini post.	TD max
M. g.	95.7–114.6; 105.1 [4]	44.7–48.7; 46.2 [3]	46.5–47.8; 47.2 [2]	51.4–56.4; 53.6 [6]	32.3–34.6; 33.4 [4]	24.9–26; 3; 25.4 [3]	59.4–63.8; 60.6 [4]
D. aff. *l.*	114–135.5[a]; 124.8 [2]	55–60.5[a]; 57.8 [2]	–	64.4	40.7	24.5–33.7; 29.1 [2]	66–77[a]; 71.5 [2]

Compared dimensions of calcanei, in mm: range; mean [number of specimens]; H: Height; post: posterior; TD: Transversal Diameter; APD: Anteroposterior Diameter; max: maximum; mini: minimum; sust.: sustentaculum tali; *M. g.*: *Mesaceratherium gaimersheimense*; *D.* aff. *l.*: *Diaceratherium* aff. *lemanense*.
[a] Measurements taken from Michel (1983).

Table 7
Mesaceratherium gaimersheimense Heissig, 1969 from Thézels, latest Oligocene, SW France.
Mesaceratherium gaimersheimense *Heissig, 1969 de Thézels, Oligocène terminal, Sud-Ouest de la France.*

				Cuboid: Prox articulation		
	L	W	H	TD	APD	Cuboid: H anterior side
Navicular	40.6–46; 44.1 [6]	34.8–37.4; 36 [6]	20.8–24.7; 22.8 [6]	–	–	–
Ectocuneiform	26.9–31.7; 29.8 [6]	36.1–45.8; 41.0 [4]	18–22.6; 20.8 [6]	–	–	–
Cuboid	48.4–55; 51.4 [5]	27.2–34.1; 31.0 [7]	41.3–45.5; 43.8 [6]	23.3–33.7; 27.8 [7]	26.6–34; 29.4 [5]	31.2–40; 35.1 [6]

Dimensions of tarsal bones, in mm: range; mean [number of specimens]; L: length; W: width; H: height; TD: transversal diameter; APD; anteroposterior diameter; prox: proximal.

narrow distal expansion. The calcaneus-facet 2 is high and triangular, with a distal lip. The calcaneus-facet 3 is an almond-shaped and transversely elongated narrow strip. All three calcaneus-facets are distinct, separate by a deep gutter.

Eight calcanei were collected. The tuber calcanei is long and thick (Fig. 6H). There is neither tibia-facet nor fibula-facet. The insertion for the *M. fibularis longus* is salient and deep, forming a deep notch trimmed by a circular ridge. The sustentaculum tali is wide (Table 6).

The navicular (eight specimens preserved) has a lozenge cross-section in vertical view (Table 7; Fig. 6I). The astragalus-facet in proximal view is concave sagittally. In distal view, the ecto-, meso-, and ento-cuneiform-facets are flat but their outline is discernible, especially on (UP.TH.2016.006).

The ectocuneiform is L-shaped in proximal (and distal) view and small (Table 7; Fig. 6J–K). The posterolateral process is weak.

On the cuboid (eight specimens; Table 7), the proximal articular surface is oval in proximal view; the astragalus- and calcaneus-facets, slightly concave sagittally, are separate by a sagittal groove. The posterior tuberosity is thick, dorsoventrally developed, and oriented postero-distally. The distal MtIV-facet is sagittally concave in distal view. The medial side shows a small navicular-facet, triangular and flat, and further separate from the astragalus-facet (Fig. 6L).

No MtII is preserved.

The MtIII is documented by two proximal epiphyses (The4113; TD = 30 mm; APD = 28 mm) and (The4304; TD = 30.4 mm; APD = 28.3 mm), pointing to a slender bone. The ectocuneiform-facet is L-shaped and slightly concave, especially near the proximal border in anterior view (Fig. 6M–N). There is no cuboid-facet. On the medial side, the anterior MtII-facet is flat. There is no posterior MtII-facet. The MtIV-facets are independent on the lateral side.

Five proximal halves of MtIV are preserved (Table 4). The4135 has a cuboid-facet flat sagittally and concave transversely (Fig. 6O–P). The postero-proximal tuberosity is restricted to a spur at the postero-lateral angle. On the medial side, the MtIII-facets are flat and independent.

3.4. Discussion

Five genera of Rhinocerotidae are known during the latest Oligocene-earliest Miocene (MP29-MN1, Fig. 7), namely *Ronzotherium* (last occurrence at MP29), *Diaceratherium*, *Mesaceratherium*, *Pleuroceros*, and *Protaceratherium* (see Scherler et al., 2013, Fig. 3). The Thézels specimens described here show size

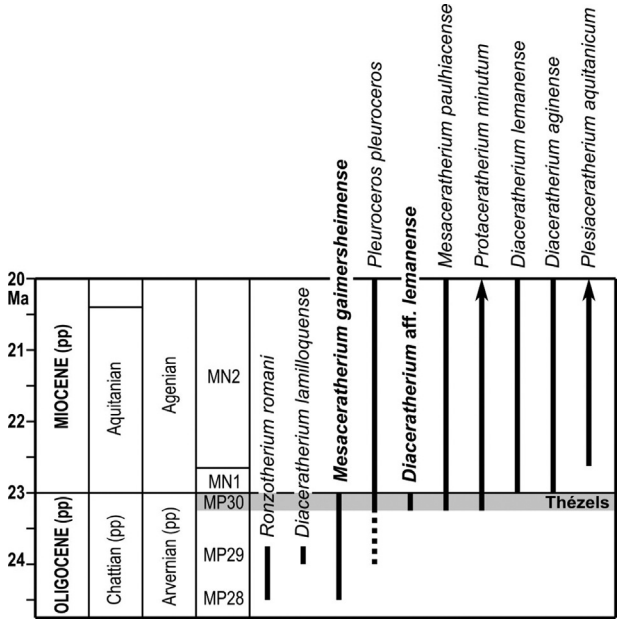

Fig. 7. Temporal distribution of rhinocerotid taxa mentioned in this study. Geologic time scale modified from Vandenberghe et al. (2012).
Distribution temporelle des rhinocérotidés cités dans cette étude. Échelle des temps modifiée de Vandenberghe et al. (2012).

differences with *D.* aff. *lemanense* (~16% on average for dental dimensions) in having slender limbs in addition to small dimensions, as mentioned by Bonis and Guinot (1987). The dental remains differ from those of *D.* aff. *lemanense*, according to our study and morphological characters listed by Antoine et al. (2010). Most differences observed between this material and that of *D.* aff. *lemanense* from Thézels are on lower cheek teeth: the V-shaped external groove, the acute dihedron-shaped trigonid and the continuous labial cingulum on lower molars (Fig. 4G–J). The comparison for upper cheek teeth of *D. lemanense* was performed thanks to the skull NMSG – P2006/1 from Eschenbach (MN2a; Becker et al., 2009). On this skull, premolars show a crochet with a crista and molars have an S-shaped central valley (crochet and antecrochet are present), whereas Thézels specimens show upper cheek teeth with a simple central valley. The complexity of the central valley on upper cheek teeth is partially observed on D4 (The4045; Fig. 2A). The current postcranial material and that described by Michel

(1983) allow to illustrate two distinct morphotypes between the stocky *D.* aff. *lemanense* and the slender rhinocerotine at Thézels. The main differences (except metric data) are observed on the astragalus. *D.* aff. *lemanense* shows an astragalus with a high collum tali and a nearly straight caudal border of the trochlea associate with a high and narrow expansion of the calcaneus-facet always present and a calcaneus-facets 2 and 3 always independent.

Dental remains of the slender rhinocerotid of Thézels, especially upper premolars, show several differences with those of *Pleuroceros pleuroceros* (Duvernoy, 1853) as a marked lingual bridge on P2, a distally directed metaloph and the absence of a connection between the protoloph and the ectoloph, and the presence of an antecrochet on P4. *Protaceratherium minutum* (Cuvier, 1822) also shows a marked lingual bridge on P2 (absent on P3 and P4), a central valley more complex on premolar with a crochet on P3, and an antecrochet on P4. Those marked differences discard any assignment of the Thézels material to *Pleuroceros*, *Protaceratherium*. The specimens studied here are distinct from those of *Plesiaceratherium* in having no strong crochet or medifossette on upper premolars (resulting from the junction of the crista and crochet), no antecrochet, crista, or long crochet on upper molars (e.g., Antoine, 2002). Moreover, dimensions of European representatives of *Plesiaceratherium* widely exceed those of Thézels remains.

On the other hand, the slender Thézels rhinocerotid shares a large number of dental characters with *M. gaimersheimense*. Indeed, global dimensions of the upper cheek teeth row are similar. Premolars show a lingual bridge on P3-P4, a hypocone stronger than the protocone and a simple central valley (absence of crochet, antecrochet or crista). Molars are quadrangular, with only an antecrochet on M1-M2, characterizing simple central valleys. Furthermore, M3 shows an ectometaloph and no constriction on the protocone in Gaimersheim and Thézels specimens. In the same way, lower cheek teeth of *M. gaimersheimense* from Gaimersheim and Toulouse-Borderouge (Antoine et al., 2006) also show close affinities with Thézels specimens: a V-shaped external groove, associated with a continuous labial cingulum on p4-m2, an angular trigonid forming an acute dihedron, and an oblique hypolophid. In terms of morpho-anatomy, size, and proportions, the Thézels specimens closely match those of *M. gaimersheimense* whenever directly comparable (mandible, upper, lower, and milk dentition; Heissig, 1969; Antoine et al., 2006). The only discrepancies between the Thézels remains and those from Gaimersheim (Heissig, 1969) and Toulouse-Borderouge (Antoine et al., 2006) are the absence of crochet on P2-P4, a continuous metaloph on M1 and M2 (The4022 and The4023; Fig. 3C–F), and a p2 with a posterior valley usually closed (Fig. 4F). We interpret these differences as low-ranged intraspecific variation.

Overall dental similarity strongly supports the referral of this rhinocerotid to *M. gaimersheimense*, as suggested by Bonis and Guinot (1987). By that time, no postcranial elements had been referred to as *M. gaimersheimense* (see Heissig, 1969), so the material available had not been included in the previous studies on Thézels rhinocerotids (Bonis and Guinot, 1987).

M. gaimersheimense as documented in Thézels displays all diagnostic characters of *Mesaceratherium*, found in *M. paulhiacense* and *M. welcommi* (see emended diagnosis here above): a transverse metaloph on P2, a strong paracone fold on M1-M2, a lingual cingulum on lower premolars, a curved magnum-facet on McII, a posterior McIII-facet on McII but no posterior MtII-facet on MtIII (as notably stated by Antoine et al., 2010). The Thézels remains add to the knowledge of *M. gaimersheimense* in providing for the first time information on most elements of the appendicular skeleton. Then, if we consider its hypodigm as a whole, *M. gaimersheimense* shows differences with other species assigned to *Mesaceratherium*. First, it differs from *M. paulhiacense* as described by Richard (1937) or Bonis (1973) in having a strongly upraised mandibular symphysis, a hypocone stronger than the protocone on P2, a lingual bridge on P3 and P4, upper molars without crochet, M1 and M2 with a continuous metaloph, and M2 without a mesostyle. In the same way, several postcranial differences between *M. gaimersheimense* and *M. paulhiacense* allow for distinguishing them. The semilunate of *M. gaimersheimense* show an acute border of the anterior side and articular-facets show a different conformation of the carp joint (*M. paulhiacense* shows a wider pyramidal-facet and a magnum-facet significantly reduced). The pisiform of *M. paulhiacense* is thicker than Thézels specimens and the medial face is less concave. The McIII of *M. gaimersheimense* (The4122) is shorter and wider than *M. paulhiacense* (Ph1018; Bonis, 1973). Moreover, on the McIII of *M. paulhiacense*, the magnum-facet is slightly marked on the dorsal face and the McII-facet is slightly inclined (Bonis, 1973). The astragalus of *M. gaimersheimense* has an APD/H ratio less than 0.65 and the orientation trochlea/distal articulation is very oblique. Furthermore, the MtIII show a concave proximal border of the anterior side with a sagittal elongation and medio-lateral constriction. These differences illustrate a more marked cursorial adaptation for *M. paulhiacense*. Indeed, *M. gaimersheimense* Heissig, 1969 had been considered as a junior synonym of *M. paulhiacense* (Richard, 1937) by several authors (e.g., Antoine et al., 2006), prior to the description of a new species assigned to *Mesaceratherium* (Antoine et al., 2010). This species, from the earliest Miocene of Pakistan, is *M. welcommi* Antoine and Downing, 2010, documented by abundant cranio-mandibular, dental and postcranial remains (Antoine et al., 2010). Comparison between *M. gaimersheimense* and *M. welcommi* highlights new morpho-anatomical differences, furthering those listed by Antoine et al. (2010): *M. gaimersheimense* differs from *M. welcommi* in having no coronary cement, a longer premolar series, a transversal metaloph (distally oriented for *M. welcommi*; Antoine et al., 2010), no lingual bridge on P2, and no constriction of the protocone on P3-P4 and M1-M2. *M. gaimersheimense* also has an angular trigonid forming an acute dihedron, no vertical external rugosities on p2-p3, an entoconid joined to the hypolophid, a continuous labial and lingual cingulum on lower premolars, and a transverse hypolophid on lower molars. Moreover, *M. gaimersheimense* differs from *M. welcommi* in having a superficial mediodistal gutter on the tibia, a closed diaphysis/olecranon angle, independent calcaneus-facet 2 and 3 on the astragalus, and no fibula-facet on the calcaneus.

4. Conclusions

Thézels (MP30) yields among the very last Oligocene mammalian faunas in France, just prior to the Oligocene-Miocene transition, as suggested by Bonis and Guinot (1987) and Comte (2000). Regarding rhinocerotids, this assemblage records the last occurrence of *M. gaimersheimense* Heissig, 1969, a rhinocerotine mostly known from Germany and France (Fig. 7). For the first time, Thézels allows for characterizing most postcranial traits of this species, which were only optimized by phylogenetic reconstruction thus far (Antoine et al., 2010). This species is a good marker for the late Oligocene and it is now recognizable through most dental and postcranial features. It is fully replaced by *Mesaceratherium paulhiacense* (Richard, 1937) after the Oligocene-Miocene transition (Antoine and Becker, 2013), even if the latter taxon has been recognized in a locality assigned to the MP30 reference level, coeval to Thézels, and named Toulouse Borderouge (Antoine et al., 2006). Accordingly, both species have virtually co-existed in SW France during the latest Oligocene interval (Fig. 7). Based on dental and postcranial differences as discussed above, both species are considered as valid. So is *Mesaceratherium welcommi* Antoine and

Downing, 2010, from the earliest Miocene of Pakistan. All three assigned species are interpreted as being browsers and cursorial forest dwellers. Noteworthy is the fact that *M. paulhiacense* has longer and slenderer autopods than *M. gaimersheimense* and *M. welcommi*, traducing a more marked cursorial locomotor mode for the former species.

Thézels also yields a medium-sized teleoceratine rhinocerotid, here referred to as *D.* aff. *lemanense*, i.e. prefiguring *D. lemanense* (Pomel, 1853), another conspicuous element of the earliest Miocene faunas of France, Germany, and Switzerland (Agenian ELMA: MN1–MN2; Antoine and Becker, 2013). A hippo-like lifestyle is suspected for *D. lemanense*, with an autopodial morphology pointing to wetlands nearby ponds or rivers (Antoine and Becker, 2013; Scherler et al., 2013).

In being restricted to two species (*D.* aff. *lemanense* and *M. gaimersheimense*), the rhinocerotid assemblage from Thézels strikingly contrasts with the geographically close and far more species-rich Paulhiac (MN1) and Laugnac (MN2) faunas. The latter localities yield widely homotaxic rhinocerotid guilds, with *Pleuroceros pleuroceros*, *P. minutum*, *M. paulhiacense*, *D. lemanense*, and *D. aginense*; Laugnac further yields *Plesiaceratherium aquitanicum* (Bonis, 1973; Boada-Saña et al., 2008; Antoine and Becker, 2013). In other words, the Thézels (MP30) – Paulhiac (MN1) – Laugnac (MN2) sequence provides a particularly well-documented series for the latest Oligocene – earliest Miocene interval, in the type area of the Agenian ELMA.

Disclosure of interest

The authors declare that they have no competing interest.

Acknowledgements

The authors are particularly grateful to the Bord family and the W. Gorbenko family. This manuscript has benefited from the wise and constructive remarks of the reviewers, Oscar Sanisidro and Luca Pandolfi. POA would like to thank Emmanuel Robert and Yves Laurent for having provided access to the collections of the Université Claude Bernard Lyon and of the Muséum de Toulouse, respectively. This work has received financial support by the Université de Poitiers and the CNRS (UMR 7262–IPHEP).

Appendix A. Supplementary Information

Rhinocerotidae (Mammalia, Perissodactyla) from the latest Oligocene of Thézels, SW France by Maxime Blanchon, Pierre-Olivier Antoine, Cécile Blondel, Louis de Bonis.

Systematic Paleontology

Order Perissodactyla Owen, 1848.
Family Rhinocerotidae Gray, 1821.
Subfamily Rhinocerotinae Gray, 1821.
Genus ***Mesaceratherium*** Heissig, 1969.
Mesaceratherium gaimersheimense Heissig, 1969.

Studied material

Old collection

Left maxilla with P2-M3 (The4022); right maxilla with P2-M2 and damaged M3 (The4023); right maxilla fragment with P2-P3 (The4026); right maxilla fragment with P3-P4 (The4027); maxilla (The4029); right maxilla fragment with M1-M3 (The4030); maxilla with right P2-M3 and fragment of left P3-M3 (The4031); damaged I1 (The4062); right I1 (The4063); left I1 (The4064); right I1 (The4065); right I1 (The4066); left I1 (The4067); right I1 (The4068); right I1 (The4305); left I1 (The4306); damaged I1 (The4308); left I1 (The4443); right I1 (The4449); upper premolar (The4040); upper premolar (The4041); right P2 (The4033); left P2 (The4036); fragment of right P2 (The4037); damaged P3 (The4033); damaged P3 (The4034); left P3 (The4038); left P4 (The4042); left P4 (The4043); fragment of left M1 or M2 (The4044); right M1 or M2 (The4047); right M1 or M2 (The4048); M1 or M2 (The4050); right M1 (The4051); left M2 (The4046); right M2 (The4049); right M3 (The4052); left M3 (The4053); fragment of right M3 (The4054); fragment of left M3 (The4055); left hemimandible with p2-m2 and m3 germ (The4001); left hemimandible from a juvenile with dp2-dp4 and preserved ramus (The4004); fragment of a right hemimandible with p4-m2 (The4005); right hemimandible with p4 and m2-m3 (The4006); fragment of a right hemimandible with m1-m2 (The4007); Fragment of a left hemimandible with m2-m3 (The4008); fragment of a left hemimandible with p4-m3 (The4009); mandibular fragment with a broken molar (The4010); fragment of a right hemimandible with p3-m2 (The4012); fragment of a right hemimandible with p4-m2 (The4013); fragment of a right edentulous hemimandible (The4015); fragment of a left hemimandible with p4-m2 (The4017); fragment of a right edentulous hemimandible (The4018); fragmentary mandible with a broken molar (The4019); fragment of a right hemimandible with p3-m3 (the4021); left mandible from a juvenile with dp2-dp4 and m1 (The4024); edentulous mandibular fragment (The4025); fragmentary mandible with m3 and a part of ramus (The4392); left dp4 (The4003); right dp4 (The4056); right i1 (The4076); right i1 (The4310); right i2 (The4087); right i2 (The4088); left i2 (The4090); left i2 (The4091); left i2 (The4092); left p1 (The4074); left p1 (The4075); right p1 (The4093); right p1 (The4307); left p1 (The4311); right p2 (The4061); right p2 (The4069); left p2 (The4070); right p3 (The4071); right p3 (The4072); right p3 (The4073); right m3 (The4002); right humerus without proximal epiphysis (The4312); distal epiphysis of humerus (The4313); distal epiphysis of right humerus (The4314); distal epiphysis of humerus (The4315); distal epiphysis of humerus (The4316); distal epiphysis of right humerus (The4318); distal epiphysis of right humerus (The4319); left humerus without proximal epiphysis (The4320); proximal epiphysis of humerus (The4321); right humerus (The4322); distal epiphysis of right humerus (The4339); distal epiphysis of humerus (The4340); distal half of left humerus (The4358); distal epiphysis of humerus (The4394); proximal epiphysis of humerus (The4408); (proximal?) epiphysis of humerus (The4423); distal epiphysis of humerus (The4424); right humerus (The4436); proximal epiphysis of right radius (The4328); proximal epiphysis of right radius (The4329); distal epiphysis of right radius (The4331); distal epiphysis of left radius (The4332); fragment of proximal epiphysis of radius (The4334); distal epiphysis of left radius (The4335); proximal epiphysis of right radius (The4337); distal epiphysis of right radius (The4398); proximal epiphysis of left radius (The4402); distal epiphysis of right radius (The4403); right proximal epiphysis of radius (The4463); left scaphoid (The4203); right scaphoid (The4204); right scaphoid (The4205); right scaphoid (The4206); right scaphoid (The4207); right scaphoid (The4208); right scaphoid (The4401); right semilunate (The4188); right semilunate (The4189); left semilunate (The4190); left semilunate (The4191); right semilunate (The4192); right semilunate (The4193); right semilunate (The4194); left semilunate (The4196); right semilunate (The4197); right semilunate (The4198); right semilunate (The4199); right semilunate (The4200); right semilunate (The4201); right semilunate (The4202); left pyramidal (The4164); left pyramidal (The4165); left pyramidal (The4166); right pyramidal (The4167); right pyramidal left pyramidal (The4168); left pyramidal (The4169); left pyramidal (The4170); right pyramidal (The4171); fragment of pyramidal (The4397);

left pyramidal (The4415); fragment of right pisiform (The4431); right pisiform (The4462); left trapezoid (The4234); right trapezoid (The4235); left trapezoid (The4237); left trapezoid (The4238); right magnum (The4172); left magnum (The4173); left magnum (The4174); left magnum (The4175); left magnum (The4176); right magnum (The4177); right magnum (The4178); left magnum (The4179); left magnum (the4180); fragment of magnum (The4400); right magnum (The4461); left unciform (The4209); left unciform (The4210); right unciform (The4211); right unciform (The4212); right unciform (The4213); left unciform (The4214); right unciform (The4215); left unciform (The4216); right unciform (The4217); right unciform (The4218); right unciform (The4219); right unciform (the4421); right unciform (The4446); right McII (The4110); proximal fragment of right McII (The4124); left McIII (The4096); left McIII (The4097); left McIII (The4098); left McIII (The4106); proximal fragment of right McIII (The4109); right McIII (The4121); right McIII (The4122); proximal fragment of McIII (The4130); left McIII (The4133); proximal half of right McIV (The4117); femur without distal end (The4341); proximal fragment of femur (The4342); distal half of right femur (The4343); distal ends of right femur (The4344); proximal half of left femur (The4345); distal fragment of left femur (The4346); distal fragment of right femur (The4347); proximal half of left femur (The4348); distal half of left femur (The4349); femoral head (The4395); right femur (The4437); right femur (The4438); left tibia (The4350); distal half of left tibia (The4351); (distal?) fragment of tibia (The4352); proximal fragment of left tibia (The4354); fragment of right tibia (The4355); distal epiphysis of left tibia (The4356); left tibia without distal end (The4357); right astragalus (The4138); left astragalus (The4139); left astragalus (The4140); fragment of astragalus (The4141); left astragalus (The4142); fragment of trochlea of astragalus (The4143); right astragalus (The4144); left astragalus (The4145); right astragalus (The4146); left astragalus (The4147); right astragalus (The4148); left astragalus (The4149); left astragalus (The4150); left astragalus (The4151); right astragalus (The4152); right astragalus (The4153); right astragalus (The4154); left astragalus (The4155); right astragalus (The4156); right astragalus (The4157); left astragalus (The4158); right astragalus (The4251); right astragalus (The4375); right astragalus (The4396); left astragalus (The4440); right astragalus (The4444); right astragalus (The4452); right calcaneus (The4159); left calcaneus (The4160); right calcaneus (The4161); right calcaneus (The4162); left calcaneus (The4163); left calcaneus (The4407); left calcaneus (The4425); left calcaneus (The4453); left navicular (The4220); right navicular (The4221); right navicular (The4222); left navicular (The4223); right navicular (The4224); right navicular (The4225); right navicular (The4226); left navicular (The4227); left ectocuneiform (The4228); left ectocuneiform (The4229); left ectocuneiform (The4230); right ectocuneiform (The4231); right ectocuneiform (The4232); right ectocuneiform (The4233); right cuboid (The4181); left cuboid (The4182); left cuboid (The4183); right cuboid (The4184); right cuboid (The4185); right cuboid (The4186); right cuboid (The4187); left cuboid (The4412); proximal epiphysis of right MtIII (The4113); proximal epiphysis of right MtIII (The4304); fragment of proximal epiphysis of left MtIV (The4095); fragment of proximal epiphysis of left MtIV (The4102); fragment of proximal epiphysis of right MtIV (The4105); fragment of proximal epiphysis of right MtIV (The4135); fragment of proximal epiphysis of right MtIV (The4137).

New collection

Proximal epiphysis of McII (UP.TH.2016.001); distal epiphysis of third metapodial (UP.TH.2016.002); left unciform (UP.TH.2016.003); tooth fragment (UP.TH.2016.004); right DP1 (UP.TH.2016.005); right navicular (UP.TH.2016.006); fragment of magnum (UP.TH.2016.007); fragment of upper cheek tooth (UP.TH.2016.008); right calcaneus (UP.TH.2016.009); complete mandible with left p2-p4/m2-m3 and right p3-p4 and m3 (UP.TH.2016.011); left calcaneus (UP.TH.2016.012); proximal epiphysis of right radius (UP.TH.2016.014); fragment of astragalus (UP.TH.2016.015).

References

Abel, O., 1910. Kritische Untersuchungen über die paläogenen Rhinocerotiden Europas. Abhandlungen der Geologische Reichsanstall, Wien 20, 1–52.

Antoine, P.-O., Welcomme, J.-L., 2000. A new rhinoceros from the Bugti Hills, Baluchistan, Pakistan: the earliest elasmotheriine. Palaeontology 43, 795–816.

Antoine, P.-O., 2002. Phylogénie et évolution des Elasmotheriina (Mammalia Rhinocerotidae). Mémoires du Muséum National d'Histoire Naturelle 188, 1–359.

Antoine, P.-O., Becker, D., 2013. A brief review of Agenian rhinocerotids in Western Europe. Swiss Journal of Geosciences 106, 135–146.

Antoine, P.-O., Duranthon, F., Hervet, S., Fleury, G., 2006. Vertébrés de l'Oligocène terminal (MP30) et du Miocène basal (MN1) du métro de Toulouse (SW de la France). Comptes Rendus Palevol 5, 875–884.

Antoine, P.-O., Downing, K.F., Crochet, J.-Y., Duranthon, F., Flynn, L.J., Marivaux, L., Métais, G., Rajpar, A.R., Roohi, G., 2010. A revision of *Aceratherium blanfordi* Lydekker, 1884 (Mammalia: Rhinocerotidae) from the early Miocene of Pakistan: postcranials as a key. Zoological Journal of the Linnean Society 160, 139–194.

Becker, D., Antoine, P.-O., Maridet, O., 2013. A new genus of Rhinocerotidae (Mammalia, Perissodactyla) from the Oligocene of Europe. Journal of Systematic Palaeontology 11, 947–972.

Becker, D., Bürgin, T., Oberli, U., Scherler, L., 2009. *Diaceratherium lemanense* (Rhinocerotidae) from Eschenbach (eastern Switzerland): Systematics, palaeoecology, palaeobiogeography. Neues Jahrbuch für Geologie und Paläontologie Abhandlungen 254, 5–39.

Boada-Saña, A., Hervet, S., Antoine, P.-O., 2008. Nouvelles données sur les rhinocéros fossiles de Gannat (Allier, limite Oligocène-Miocène). Revue des Sciences Naturelles d'Auvergne 71, 1–25.

de Bonis, L., 1973. Contribution à l'étude des mammifères de l'Aquitanien de l'Agenais. Rongeurs-Carnivores-Périssodactyles. Mémoires du Muséum National d'Histoire Naturelle 28, 1–192.

de Bonis, L., Guinot, Y., 1987. Le gisement de Vertébrés de Thézels (Lot) et la limite Oligo-Miocène dans les formations continentales du bassin d'Aquitaine. Münchner Geowissenschaftliche Abhandlungen 10, 49–57.

Brunet, M., de Bonis, L., Michel, P., 1987. Les grands Rhinocerotidae de l'Oligocène supérieur et du Miocène inférieur d'Europe occidentale : intérêt biostratigraphique. Münchner Geowissenschaftliche Abhandlungen 10, 59–66.

Cavaillé, A., 1981. Les calcaires lacustres du Bas-Quercy. Bulletin de la société de sciences naturelles du Tarn & Garonne 12, 1–30.

Comte, B., 2000. Rythme et modalités de l'évolution chez les rongeurs à la fin de l'Oligocène : Leurs relations avec les changements de l'environnement. Palaeovertebrata 29 (2–4), 83–360.

Cuvier, G., 1822. Recherches sur les ossements fossiles de quadrupèdes, vol 5. Edmond d'Ocagne, Paris.

Depéret, C., Douxami, H., 1902. Les vertébrés oligocènes de Pyrimont-Challonges (Savoie). Kündig [vol. 29, No. 1].

Dietrich, W.O., 1931. Neue Nashornreste aus Schwaben (*Diaceratherium tomerdingensis* n. g. n. sp.). Zeitschrift für Säugetierkunde 6, 203–220.

Duvernoy, G.L., 1853. Nouvelles études sur les rhinocéros fossiles. Archives du Muséum d'Histoire Naturelle, Paris 7, 1–144.

Heissig, K., 1969. Die Rhinocerotidae (Mammalia) aus der oberoligozänen Spaltenfüllung von Gaimersheim bei Ingolstadt in Bayern und ihre phylogenetische Stellung. Abhandlungen der Bayerischen Akademie der Wissenschaften 138, 1–133.

Nouel, A., 1866. Mémoire sur un nouveau Rhinocéros fossile. Mémoires de la Société d'Agriculture, des Sciences, des Belles Lettres et des Arts d'Orléans, 8., pp. 1–13.

Pomel, M., 1853. Catalogue méthodique et descriptif des vertébrés fossiles découverts dans le bassin hydrographique supérieur de la Loire, et surtout dans la vallée de son affluent principal, l'Allier. Baillière, Paris, pp. 1–193.

Michel, P., 1983. Contribution à l'étude des Rhinocerotidae oligocènes : (La Milloque; Thézels; Puy de Vaurs). Université de Poitiers. Thèse 3e cycle 926 [Inédit].

Répelin, J., 1917. Etudes paléontologiques dans le sud-ouest de la France (Mammifères). Les Rhinocerotidae de l'Aquitanien supérieur de l'Agenais (Laugnac). Annales du Muséum d'Histoire naturelle de Marseille 16, 1–47.

Richard, M., 1937. Une nouvelle espèce de Rhinocérotidé aquitanien : *Diaceratherium pauliacensi*. Bulletin de la Société d'Histoire Naturelle de Toulouse 71, 165–170.

Richard, M., 1948. Contribution à l'étude du Bassin d'Aquitaine. Les gisements de Mammifères tertiaires. Mémoires de la Société Géologique de France 24, 1–348.

Roger, O., 1898. Wirbeltierreste aus dem Dinotheriensande der bayerisch-schwäbischen Hochebene. Bericht des Naturwissenschaftlichen Vereins für Schwaben und Neuburg 33, 383–396.

Scherler, L., Mennecart, B., Hiard, F., Becker, D., 2013. Evolutionary history of hoofed mammals during the Oligocene-Miocene transition in Western Europe. Swiss Journal of Geosciences 106 (2), 349–369.

Vandenberghe, N., Hilge, F., Speijer, R., 2012. The Paleogene Period. In: Gradstein, F., Ogg, J., Schmitz, M., Ogg, G., et al. (Eds.), The Geologic Time Scale. Boston, Elsevier [Chap. 2, pp. 855–921].